07

The limiting energy capabilities of high−power AlInGaN LEDs

© A.L. Zakgeim[1], A.V. Aladov[1], A.E. Ivanov[1,2], N.A. Talnishnikh[1], A.E. Chernyakov[1]

[1] Submicron Heterostructures for Microelectronics, Research & Engineering Center, RAS, Saint-Petersburg, Russia
[2] Petersburg State Electrotechnical University „LETI", St. Petersburg, Russia
E-mail: zakgeim@mail.ioffe.ru

Received March 2, 2022
Revised May 5, 2022
Accepted May 16, 2022

The object of study in this work was the most advanced AlInGaN LEDs of the „UX:3" design with a distributed system of reflective contacts located on the back side of the emitting chip. The current dependences of the output optical power and emission spectral characteristics, including their distribution (mapping) over the emitting surface in a wide range of operating currents up to ~ 30 A have been studied. An analysis of the near−field emission by intensity and spectrum revealed a high uniformity of the current density distribution at all levels of excitation (no current crowding). Thus, the saturation of the optical power and the quantum efficiency droop are explained by purely internal factors, which are well described by the *ABC* model.

Keywords: AlInGaN LED, quantum efficiency, emission spectrum, near−field emission.

DOI: 10.21883/TPL.2022.07.54033.19182

AlInGaN LEDs produced by leading manufacturers, first of all by OSRAM Opto Semiconductors, Philips Lumileds, are so far distinctively characterized by a high level of design excellence and emission characteristics. An optimized MQW-heterostructure (MQW means a multiple quantum well), a system of distributed reflective contacts, and low electric and thermal resistances have provided wattful optical powers from square millimeter of the emitting surface at a high (above 50%) efficiency [1]. Most of studies devoted to AlInGaN LEDs considered their continuous operating mode, which is quite natural because their main application is lighting. Along with this, an interest has recently increased to using AlInGaN LEDs of the visible blue−green spectral range not only „for eye" but also in working with physical receivers, for instance, in pumping solid−state lasers or in open information transmission systems of visible light communication (VLC) [2]. New applications impose requirements for LED speeds (formation of light pulses with the lengths of tens of nanoseconds to units of microseconds) and, what is more important, for the ability to reach the maximum possible emission power (pulse energy).

In [3] we have studied the behavior at high pulsed currents of AlInGaN LEDs of the „vertical" design with *p*- and *n*-contacts located on opposite sides of the emitting chip. It was established that restriction of the emission output power with increasing excitation is caused by the geometric factor, namely, current „crowding" near the *n*-contact and under it, increase in the local current density, and enhancement of light shadowing by contacts rather than by such a physical factor as the decrease in internal quantum yield η_{int} („efficiency droop") with current. In this work, we have chosen for analyzing the limiting energy capabilities of the AlInGaN LEDs the light emitting diodes of the design most advanced at this moment, namely, the so-called „UX:3" design [4,5] realized in commercial LEDs OSRAM OSTAR LE B Q8WP [6]. As Fig. 1 shows, the main distinctive feature of the „UX:3" chips is the multipoint geometry of reflecting *n*-contacts that are transferred to and uniformly distributed over the *p*-contact area on the chip back side by using the special technique of „isolated wells". The complexity of this technique is compensated by the conditions ideal for the uniform current distribution and light extraction without losses caused by shadowing. Light emission diode LE B Q8WP is an emitting chip of the „UX:3" type 1.5×1.2 mm in size which is mounted on a switching plate providing electrical contact and heat removal; the casing is protected with a glass window. According to Specifications, the nominal continuous mode current is $I = 1.4$ A (maximum permissible current is $I_{\max} = 5$ A), forward voltage is $U_f \approx 3.3$ V, nominal mode

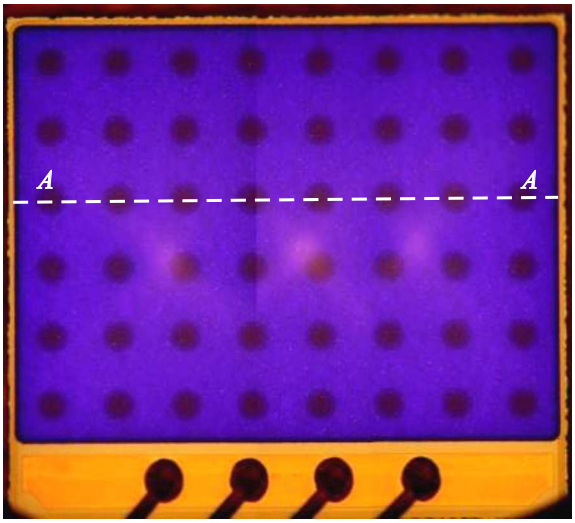

Figure 1. A photograph of the LED LE B Q8WP emitting surface. Dark circles indicate the positions of *n*-contacts.

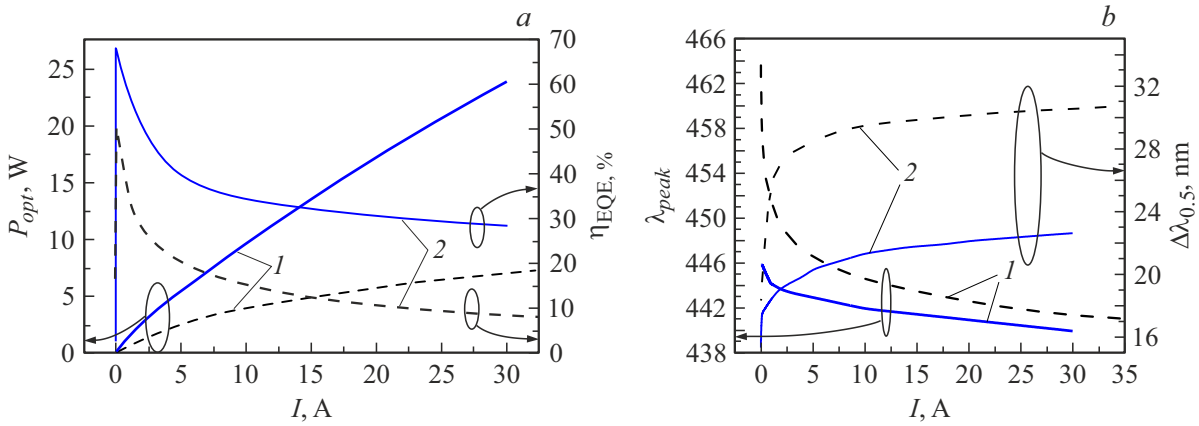

Figure 2. *a* — current dependences of the output optical power P_{opt} (*1*) and external quantum efficiency η_{EQE} (*2*); *b* — current dependences of the peak wavelength λ_{peak} (*1*) and spectrum half width $\Delta\lambda_{0.5}$ (*2*). For comparison, dashed lines in both panels represent similar dependences for „vertical" LED SemiLEDs EV-B40A [3].

emission power is $P_{opt} \approx 2$ W (hence, the design efficiency is $\approx 40\%$).

The pulsed–mode studies were performed in the pulse length range of $\tau = 100-3000$ ns at frequency $F = 100$ Hz (to prevent self–heating) and currents of up to 30 A.

Fig. 2, *a* presents current dependences of the emission power P_{opt} and external quantum efficiency η_{EQE}, while Fig. 2, *b* demonstrates current dependences of the emission peak wavelength λ_{peak} and spectrum half width $\Delta\lambda_{0.5}$ in the current range from fractions of milliampere to 30 A (with the current density of up to $J \sim 1.7$ kA/cm^2). The pulsed mode of measurements was provided by generator Agillent 8114A with amplifier PicoLAS LDP-V80-100 V3.3. The emission optical power and spectra were measured by complex „OL 770-LED High-speed LED Test and Measurement System", the sample temperature was $T = 300$ K.

Fig. 2 clearly demonstrates a significant difference in both the power and spectral characteristics of the AlInGaN LEDs of two designs, „vertical" and „UX:3". The advantage of the latter is evidenced by a smoothed (less steep) droop of η_{EQE} with current, which allows achieving at $I = 30$ A a significant optical power $P_{opt} = 24$ W (that for the „vertical" chip is only ~ 7 W). Along with this, improvement of the emission spectrum current stability is observed: for „UX:3" the „blue shift" with the current increase from 0.1 to 30 A is $\lambda_{peak(0.1\to30)} = 446-440 = 6$ nm, while the spectrum broadening is $\Delta\lambda_{0.5(0.1\to30)} = 22-15 = 7$ nm (those for the „vertical" chip are 25 and 15 nm, respectively, i. e. are 4 and 2 times higher).

To elucidate the sources of so different behaviors of LEDs having the same–type designs (MQW, remote substrate, etc.) and close initial (low–current) energy and spectral characteristics, we performed the comparative analysis of chips of two types with respect to the current and heat distribution at increasing excitation. Paper [3] has shown for the „vertical" chips that, when the current increases, the effect of its localization near the contact develops, which makes the real current density much higher than the average value matching with the $p-n$ junction area. In the case of the „UX:3" chip, the pattern is quite different. To estimate quantitatively the current density distribution over area, the chip emission near field was scanned by two coordinates with measuring the intensity and spectrum. The power and spectral mapping was carried out by using optical microscope Mitutoyo combined with spectrometer Avantes AvaSpec-2048. The optical system ensured the spatial resolution of $\sim 30\,\mu$m.

Fig. 3, *a* presents the results of scanning the emission near field along the *AA* axis (Fig. 1) in the high–resolution scale matching with the distance between the neighboring „wells" of *n*-contacts ($200\,\mu$m).

As Fig. 3, *a* shows, high uniformity of the emission intensity (within 10%) and spectrum (within $\lambda_{peak} < 1.5$ nm) retains between the *n*-contacts even at high currents, which evidences for the uniformity of the current density distribution. This is also confirmed by the emission spectra presented in Fig. 3, *b* for two characteristic points: in the middle between the contacts and at the edge of the contact. Equal slopes of the spectra shortwave shoulders $a = 0.06$ mean the absence of temperature gradients over the active region area which could occur in the case of the current localization.

Based on the mapping result that demonstrate the current distribution uniformity, we considered it correct to use in subsequent analysis of the current dependences behavior via the *ABC* model [7] the average values of current density defined as $J = I/S$ (where I is the current, S is the chip area). Within the *ABC* model, the quantum efficiency is defined through the competition between three recombination mechanisms in the active region:

$$\eta_{EQE} = \eta_{ext}\eta_{IQE} = \eta_{ext}\frac{Bn^2}{An + Bn^2 + Cn^3}. \qquad (1)$$

Here η_{IQE} is the internal quantum efficiency, η_{ext} is the emission extraction coefficient, n is the carrier concentration, A, B and C are the coefficients of the Chockley–Reed–Hall

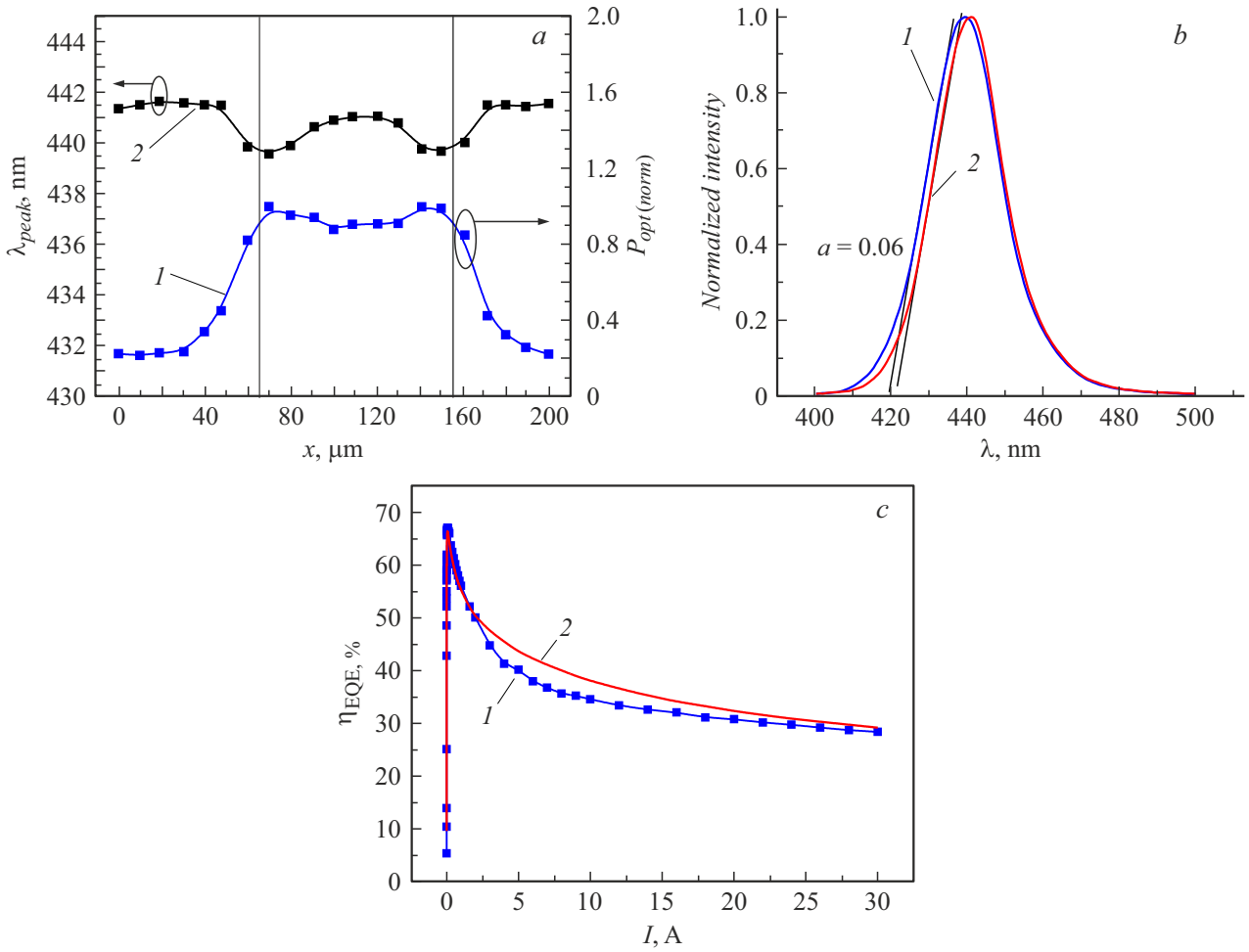

Figure 3. *a* — distribution between neighboring *n*-contacts of the emission normalized intensity $P_{opt(norm)}$ (*1*) and peak wavelength λ_{peak} (*2*) over cross–section *AA* (see Fig. 1) at current $I = 30$ A; *b* — emission spectra at two points of the emitting surface: in the middle between the contacts (*1*) and at the edge of the *n*-contact (*2*); *c* —the experimental (*1*) and designed via the *ABC* model (*2*) η_{EQE} dependences on current.

recombination, radiation biomolecular recombination, and Auger–recombination, respectively. Using the known transformations [8] in constructing experimental dependences of the reduced quantum efficiency $\eta_{EQE}^{max}/\eta_{EQE}$ on the sum of roots of reduced powers $(p^{1/2} + p^{-1/2})$, where $p = P_{out}/P_{out}^{max}$ and P_{out}^{max} is the output optical power at the current corresponding to η_{EQE}^{max}, obtain the expression for determining the basic parameters of radiative recombination

$$\eta_{EQE}^{max}/\eta_{EQE} = \eta_{IQE}^{max} + \frac{p^{1/2} + p^{-1/2}}{Q + 2}. \qquad (2)$$

Using the curve plotted based on expression (2) and its extrapolation to $(p^{1/2} + p^{-1/2}) \to 0$, it is possible to determine η_{IQE}^{max} and $Q = B/(AC)^{1/2}$ that is the „quality factor". Taking into account $\eta_{EQE} = \eta_{ext}\eta_{IQE}$ and knowing η_{IQE} and experimentally measured η_{EQE}, it is possible to determine also η_{ext}, i. e. all the primary parameters of LEDs. The results of relevant construction of the $\eta_{EQE}^{max}/\eta_{EQE}$ dependence on the $(p^{1/2} + p^{-1/2})$ combination based on the experimental dependence in the medium current section (0.1–0.5 A) have provided values $\eta_{IQE}^{max} = 0.8$, $Q = 8$, $\eta_{ext} = 0.84$.

Notice that the obtained values seem to be quite realistic: value $\eta_{IQE}^{max} = 0.8$ matches with the best values known from literature, $\eta_{ext} = 0.84$ corresponds to the perfect crystal structure free of light absorbing elements but comprising highly reflective contacts.

Fig. 3, *c* presents experimental dependence $\eta_{EQE} = f(I)$ (curve *1*) taken from Fig. 2, *a* and dependence calculated via the *ABC* model and extrapolated to the current of 30 A (curve *2*). Good agreement of the curves in a wide range of currents evidences that the design of the „UX:3" chip realizes energy characteristics close to those maximum theoretically possible at the modern level of the AlInGaN LED technology. The *ABC* model authentically describes the output optical power saturation with current in connection with „internal" physical processes of recombination, while additional mechanisms of losses caused by „external" design drawbacks are almost absolutely absent.

Thus, it is possible to state with high confidence that achieved to this moment energy capabilities ($\sim 25\,W$) of the single crystal emission at the efficiency of $\sim 25\%$ ($\sim 15\,W/mm^2$) are close to the limiting ones restricted by physical principles of the AlInGaN LED operation. At the same time, these parameters are quite high even relative to those of injection „blue-green AlInGaN lasers and are sufficient for solving a number of new problems, for instance, optical pumping of solid−state lasers.

Acknowledgements

The LED parameters were studied at CCU „Hardware components for radiophotonics and nanoelectronics: technology, diagnostics, metrology".

Conflict of interests

The authors declare that they have no conflict of interests.

References

[1] S.Yu. Karpov, Proc. SPIE, **9768**, 97680C (2016). DOI: 10.1117/12.2207265
[2] P. Pichon, A. Barbet, J.-P. Blanchot, F. Druon, F. Balembois, P. Georges, Optica, **5** (10), 1236 (2018). DOI: 10.1364/OPTICA.5.001236
[3] A.L. Zakgeim, A.E. Ivanov, A.E. Chernyakov, Tech. Phys. Lett., **47**, 834 (2021). DOI: 10.1134/S1063785021080290
[4] A. Laubsch, M. Sabathil, J. Baur, M. Peter, B. Hahn, IEEE Trans. Electron Dev., **57** (1), 79 (2010). DOI: 10.1109/TED.2009.2035538
[5] B. Hahn, B. Galler, K. Engl, J. Appl. Phys., **53** (10), 100208 (2014). DOI: 10.7567/JJAP.53.100208
[6] OSRAM Datasheet LE B Q8WP [Electronic source]. Available at: https://www.osram.com/ecat/OSRAM%20OSTAR%C2%AE%20Projection%20Compact%20LE%20B%20Q8WP/com/en/class_pim_web_catalog_103489/prd_pim_device_2191200/
[7] S.Yu. Karpov, Opt. Quantum Electron, **47** (6), 1293 (2015). DOI: 10.1007/s11082-014-0042-9
[8] I.E. Titkov, S.Yu. Karpov, A. Yadav, V.L. Zerova, M. Zulonas, B. Galler, M. Strassburg, I. Pietzonka, H. Lugauer, E.U. Rafailov, IEEE J. Quantum Electron., **50** (11), 911 (2014). DOI: 10.1109/JQE.2014.2359958